Coating of a layer of Au on Al_{13}: The findings of icosahedral $Al@Al_{12}Au_{20}^{-}$ and $Al_{12}Au_{20}^{2-}$ fullerenes using *ab initio* pseudopotential calculations

Vijay Kumar
Dr. Vijay Kumar Foundation, 1969 Sector 4, Gurgaon 122001, Haryana, India
(Received 26 November 2008; published 20 February 2009)

We report results of *ab initio* pseudopotential calculations on the nanocoating of gold on an icosahedral Al_{13} cluster and the findings of icosahedrally symmetric endohedral $Al@Al_{12}Au_{20}^{-}$ and empty cage $Al_{12}Au_{20}^{2-}$ compound fullerenes formed of metal atoms. Twelve Al atoms cap the pentagonal faces of a dodecahedral Au_{20} cage in which each Au atom has three Al atoms and three Au atoms as nearest neighbors. Mixing of Al_{13} and Au_{20} magic clusters leads to a large heat of formation of 0.55 eV/atom and high stability of the $Al@Al_{12}Au_{20}$ compound fullerene. The binding energies of $Al_{12}Au_{20}$ and $Al@Al_{12}Au_{20}$ are 3.017 and 3.007 eV/atom, respectively, which are much larger than 2.457 eV/atom for Au_{32} fullerene, leading to the possibility of their high abundance.

DOI: 10.1103/PhysRevB.79.085423 PACS number(s): 61.48.−c, 61.46.Bc, 71.15.Nc, 73.22.−f

I. INTRODUCTION

The discovery of carbon fullerenes[1] with cage structures created much interest in the search of similar clusters of other materials, and metallocarbohedrenes of the form M_8C_{12} (M=Ti, V, Cr, Fe, Zr, Nb, Mo, and Hf) were also reported[2] to be formed. In recent years fullerene cages of Au_{32} (Ref. 3) and B_{80} (Ref. 4) have been obtained. Boron is adjacent to carbon and several fullerene and nanotube structures have been predicted,[5] but the finding of a fullerene structure of Au_{32} as well as cage structures for some other sizes[6,7] is unusual because metal clusters often tend to be close packed and bulk gold is not a layered material. However, neutral gold clusters with up to 13 atoms are planar,[7] while Au_{20} has all the atoms on the surface of a tetrahedron.[8] Most surprisingly gold clusters exhibit good catalytic activity[9] although bulk gold is the most inert metal. Therefore gold clusters in different forms could lead to new and interesting catalytic behavior. Here we study the nanocoating of gold on an Al_{13} cluster and report a 14 carat fullerene cage of $Al_{12}Au_{20}$.

Clusters of *s-p* bonded metals such as Na and K are known[10,11] to exhibit electronic shell closure for 8, 20, 40, 58,… valence electrons and such clusters have been referred to as magic clusters. For aluminum clusters, Al_{13}^{-} with 40 valence electrons is particularly stable with a large highest occupied molecular orbital–lowest unoccupied molecular orbital (HOMO-LUMO) gap[12] and high abundance.[13] Nanocoating of such magic clusters of cheap materials could provide a novel way to design new catalysts, reduce cost, and find new species. Traditionally gold plating has been and is widely used in jewelry and other forms in bulk. It is of interest to explore what happens when gold is plated on nanoparticles as nanoform gold is quite different from bulk.

Earlier studies[11,14] on Al_{13} have shown that it has an icosahedral structure with 20 triangular faces. We coat this cluster with 20 Au atoms, one on each triangular face. Incidentally as an isolated aggregate Au_{20} is also a magic cluster with a tetrahedral structure and a large HOMO-LUMO gap,[8] but we find that nanocoating of 20 gold atoms on Al_{13} is highly exothermic with respect to the energies of Al_{13} and Au_{20} clusters. There is a formation of a compound fullerene with an endohedral cage structure that has a nearly spherical shape and an Al atom inside. Removal of this Al atom shows the existence of a fullerene cage of $Al_{12}Au_{20}$ and an electronically closed shell $Al_{12}Au_{20}^{2-}$ species with 58 valence electrons leaving aside the $5d$ electrons of gold.

In Sec. II we present the method of calculations, while the results are discussed in Sec. III. A summary and concluding remarks are given in Sec. IV.

II. METHOD OF CALCULATIONS

The calculations have been performed using the *ab initio* projector augmented wave (PAW) pseudopotential plane-wave method.[15] The ionic potential has been generated by including scalar relativistic effects. The exchange-correlation energy has been calculated within the generalized gradient approximation.[16] We consider 3 and 11 valence electrons for Al and Au, respectively, and the cutoff energy for the plane-wave expansion is taken to be 240.437 eV. The cluster is placed in a large cubic unit cell of 20 Å sides, and the Brillouin-zone integrations are performed using only the Γ point. A neutralizing background has been used for the charged clusters. Spin-polarized calculations have been performed in case that there are an odd number of electrons in the cluster. The atomic structures are optimized without any symmetry constraints, and the absolute value of force on each ion is brought to less than 0.01 eV/Å. The energy convergence is achieved within 10^{-5} eV. Calculations on Al_2, Au_2, and AlAu dimers give the binding energies (BEs), defined with respect to neutral free atoms, as 0.931, 1.155, and 1.887 eV/atom and the bond lengths as 2.49, 2.52, and 2.36 Å, respectively. The Al_2 dimer has $2\mu_B$ magnetic moment, while Au_2 and AlAu are nonmagnetic. The AlAu and Au_2 dimers have large HOMO-LUMO gaps of 2.42 and 1.98 eV, respectively. Accordingly the bond between Al and Au atoms is very strong and it is expected that the combined Al-Au cluster would tend to optimize the Al-Au bonds.

III. RESULTS

A. Atomic structures of $Al@Al_{12}Au_{20}^{-}$ and $Al_{12}Au_{20}^{2-}$

Figures 1(a) and 1(b) show the optimized structures of the magic clusters, Al_{13}^{-} and Au_{20}, which have high symmetry,

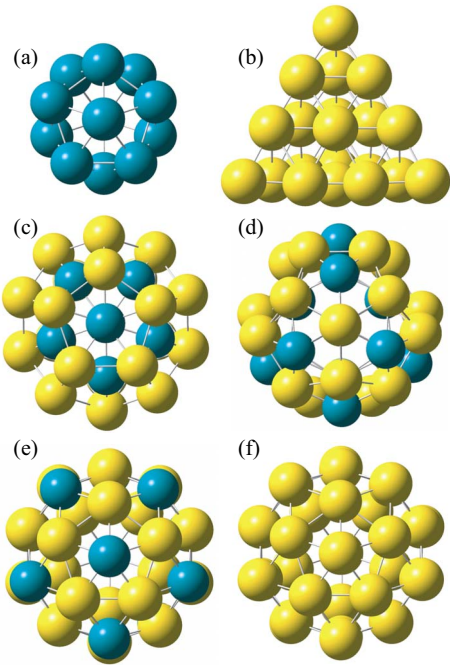

FIG. 1. (Color online) Atomic structures of (a) Al_{13}^- and (b) Au_{20}. (c) and (d) show two isomers of $Al_{13}Au_{20}^+$, (d) being lower in energy. (e) and (f) show icosahedrally symmetric $Al@Al_{12}Au_{20}^-$ and Au_{32}, respectively. The yellow (light gray) and blue (dark gray) balls show Au and Al atoms, respectively.

large HOMO-LUMO gaps of 1.88 and 1.78 eV, respectively, and high stability. Also shown are two isomers of the $Al_{13}Au_{20}^+$ cluster which has 58 valence electrons without the 5*d* electrons of gold: (i) one in which 20 gold atoms are coated on Al_{13}, one each on a triangular face so that gold atoms form a dodecahedral fullerene shell such that the Al_{13} icosahedral cluster remains nearly intact inside the gold shell [Fig. 1(c)], and (ii) another in which there is a compound formation such that 10 Al atoms come out of the pentagons of the dodecahedral fullerene gold cage [Fig. 1(d)]. The central Al atom inside the cage is slightly displaced from the center and interacts strongly with two Al atoms that lie slightly inside the cage. We find that isomer (ii) lies 4.03 eV lower in energy than isomer (i), and therefore it is energetically highly favorable. Note that in bulk also Al-Au alloys have strong ordering tendency with negative heat of formation and a compound with composition Al_2Au exists.[17] Further calculations on neutral and anion clusters of isomer (ii) show that the neutral cluster is only slightly distorted from perfect icosahedral symmetry with all the 12 Al atoms capping the pentagonal faces of the gold dodecahedral fullerene in which the Au-Au bonds vary between 2.80 and 2.86 Å. The HOMO-LUMO gap obtained from spin-polarized calculations is 0.23 eV. The anion cluster $Al_{13}Au_{20}^-$ is, however, an icosahedrally symmetric endohedral fullerene $Al@Al_{12}Au_{20}^-$ as shown in Fig. 1(e), very similar to the Au_{32} fullerene cage [Fig. 1(f)], but with an Al atom at the center. In this anion structure each Au atom is sixfold coordinated with three nearest-neighbor Al atoms at a distance of 2.60 Å and three gold atoms at a distance of 2.80 Å. Each capping Al atom has five Au atoms in the pentagonal face as nearest neighbors

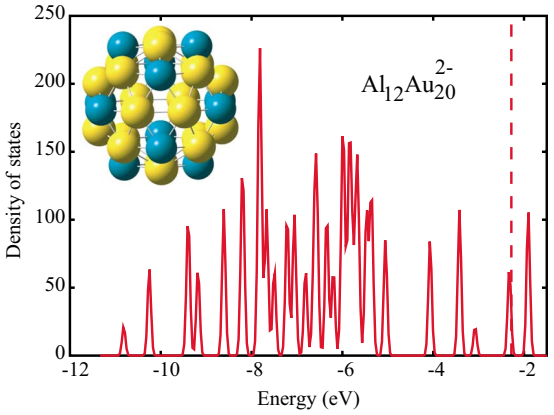

FIG. 2. (Color online) Gaussian broadened (half-width: 0.05 eV) electronic states of $Al_{12}Au_{20}^{2-}$. The broken line shows the HOMO. The atomic structure of the empty center fullerene cage is shown in the inset with yellow (light gray) and blue (dark gray) balls representing Au and Al atoms, respectively.

at a distance of 2.60 Å. The central Al atom is 4.16 Å (3.92 Å) apart from the other Al (Au) atoms on the cage as compared to the center to vertex bond length of 2.66 Å in the Al_{13}^- cluster. Therefore the chemical bond between the central Al atom and the cage is weak. We also displaced the central Al atom from the center in order to find if this atom would prefer to bind with the inner wall of the cage. However, after reoptimizaton, it comes back to the center.

The BE of the neutral $Al@Al_{12}Au_{20}$ is 3.007 eV/atom as compared to the values of 2.685, 2.337, and 2.457 eV/atom for Al_{13}, Au_{20}, and Au_{32}, respectively. Therefore, $Al@Al_{12}Au_{20}$ is highly stable and energetically very favorable as compared to the elemental Al and Au clusters of similar sizes. Also all the atoms in the fullerene are highly undercoordinated compared with atoms in bulk Al and bulk Au which have 12 coordination in the face-centered-cubic structure. However, the BE in the fullerene structure is already about 73% of the atomic fraction–weighted experimental value of 3.7 eV/atom taking the experimental cohesive energies of 3.39 and 3.9 eV/atom for bulk Al and Au, respectively. The heat of formation, $\Delta E = E(Al@Al_{12}Au_{20}) - E(Al_{13}) - E(Au_{20})$, of the compound fullerene from the constituent Al_{13} and Au_{20} clusters is 0.55 eV/atom which is quite high and suggests strong stability of this fullerene. Here $E(X)$ is the total energy of the species X. The electron affinity of $Al@Al_{12}Au_{20}$ is 3.326 eV, and it is comparable to the value of 3.777 eV for Al_{13}. Therefore high abundance of the anion $Al@Al_{12}Au_{20}^-$ fullerene is very likely.

As the chemical interaction between the central Al atom and the cage is weak, we removed the central Al atom and reoptimized the cage which is found to remain stable. The neutral cage has 56 valence electrons excluding the 5*d* electrons on Au atoms. We therefore charged it with two electrons and found a highly symmetric icosahedral fullerene cage of $Al_{12}Au_{20}^{2-}$ (see inset of Fig. 2). The electronic spectra of $Al_{12}Au_{20}^{2-}$ and $Al@Al_{12}Au_{20}^-$ are shown in Figs. 2 and 3, respectively, and the two are very similar. The electronic spectrum of the empty cage is slightly shifted to lower binding energy because of the extra negative charge. In the en-

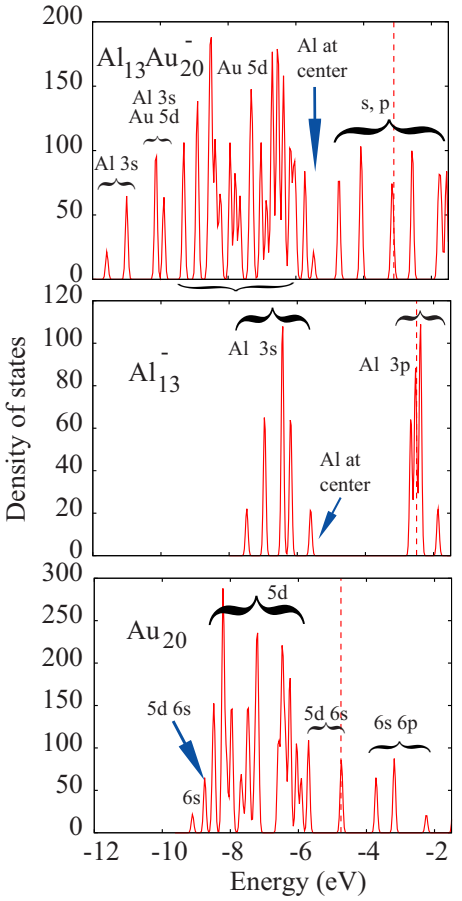

FIG. 3. (Color online) Same as in Fig. 2 but for $Al@Al_{12}Au_{20}^-$ together with the states of Al_{13}^- and Au_{20} at the same positions as in the compound fullerene.

dohedral cage there is an extra occupied level at −5.494 eV (marked by an arrow in Fig. 3) that arises predominantly from the 3*s* orbital of the central Al atom. Therefore effectively the central Al atom provides an electron to the cage (see also below). The HOMO-LUMO gaps for the empty and the endohedral symmetric cages are 0.41 and 0.55 eV, respectively. The BE of the neutral $Al_{12}Au_{20}$ cage is 3.017 eV/atom as compared to 3.007 eV/atom for $Al@Al_{12}Au_{20}$. The BEs for $Al_{12}Au_{20}^{2-}$ and $Al@Al_{12}Au_{20}^-$ are 3.193 and 3.108 eV/atom, respectively. Therefore, the empty cage is energetically slightly more favorable than the endohedral cage.

B. Electronic structure

In order to understand the electronic structure, we calculated the electronic spectra of the Al_{13}^- and Au_{20} species at the same positions of Al and Au atoms as in the compound fullerene $Al@Al_{12}Au_{20}^-$ and these are shown in Fig. 3. The Al_{13}^- spectrum separates into two blocks that have a large energy gap. The lower-lying states arise mainly from the 3*s* orbitals of Al atoms and accommodate 26 electrons, while the remaining 14 electrons are accommodated in the states arising mainly from the 3*p* orbitals. The electronic states of the dodecahedral Au_{20} have *s*-*d* hybridization at the bottom

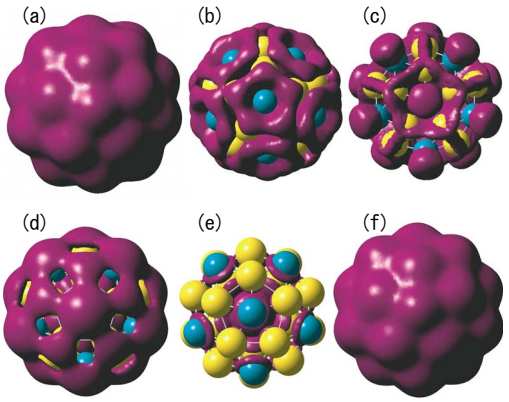

FIG. 4. (Color online) Isosurfaces of (a) the total electronic charge density of $Al@Al_{12}Au_{20}^-$ fullerene ($0.0625e/Å^3$); (b) excess charge and (c) depletion of charge ($1.25\times10^{-4}e/Å^3$) as compared to the sum of the electronic charge densities of Al_{13}^- and Au_{20} at the same positions as in the compound fullerene; (d) excess charge and (e) depletion of charge ($1.25\times10^{-4}e/Å^3$) as compared to the sum of the electronic charge densities of $Al_{12}Au_{20}$ and Al atom at the center; and (f) the total valence electronic charge density of $Al_{12}Au_{20}^{2-}$ ($0.0625e/Å^3$).

and the top of the 5*d* states as shown in Fig. 3, while the states above the HOMO are predominantly *s*-*p* hybridized. The HOMO lies in a state which is fourfold degenerate and it is partially occupied. Therefore in these positions neither Al_{13}^- nor Au_{20} has a significant HOMO-LUMO gap. In the combined spectrum of $Al@Al_{12}Au_{20}^-$, the 3*s* states of Al atoms get pulled down due to the charge transfer from Al atoms to Au sites (see below), and these lie at the bottom of the spectrum with some hybridization with the 5*d* states of Au. The 5*d* states are, however, much less affected due to interaction with Al atoms. But the part of the spectrum above the 5*d* states of Au_{20} has significant changes. In this region states derived from 3*p* orbitals of Al and the *s*-*p*-*d* orbitals of Au get mixed up. The charge transfer to Au leads to the occupation of some unoccupied states of Au_{20} and the HOMO-LUMO gap is much smaller than in the ground-state structures of Al_{13}^- and Au_{20}. Also the gap is much smaller than 1.57 eV for the Au_{32} fullerene cage. Therefore in this fullerene structure Au atoms can be expected to be more reactive as compared to the tetrahedral Au_{20} cluster or the icosahedral Au_{32} fullerene.

Figure 4 shows the isosurfaces of the total electronic charge and the difference in the electronic charge density of $Al@Al_{12}Au_{20}^-$ and the sum of the charge densities of Au_{20} and Al_{13}^-, keeping the Au and Al atoms at the same positions as in the compound fullerene. The total valence electronic charge-density isosurface shows a metallic nature of bonding. However, as shown in Figs. 4(b) and 4(c), there is charge transfer from Al atoms to Au atoms and this leads to the enhanced stability of this cage. Charge from the top of the Al atoms flows to Au atoms and it creates some covalent character in the bonds also (see excess charge in Au-Au bonds). We also calculated the difference in the electronic charge densities of $Al@Al_{12}Au_{20}^-$ and the sum of the charge densities of $Al_{12}Au_{20}$ and the Al atom at the center, keeping the same positions as in the compound fullerene

$Al@Al_{12}Au_{20}^-$, in order to understand the role of the atom at the center. The excess charge and the depletion of charge are shown in Figs. 4(d) and 4(e), respectively. It is to be noted that the compound fullerene has an extra charge and we can see excess charge on all the atoms in the cage. There is depletion of charge close to the central Al atom and some excess charge happens in between the central Al atom and the cage. This excess charge distribution has directional feature and it is pointed toward the 12 Al atoms on the cage as one can notice in Fig. 4(d). The charge-density isosurface of $Al_{12}Au_{20}^{2-}$ is also shown in Fig. 4(f) and it is quite similar to the isosurface for $Al@Al_{12}Au_{20}^-$. Although a simple jellium picture may not be directly applicable in these compound fullerenes due to charge transfer between atoms as well as the participation of 5*d* orbitals of Au in bonding, the charge distribution has metallic character and counting the Al 3*s*-3*p* states as well as the Au *s*-*p* valence states, the stability of these structures can be effectively correlated with 58 valence electron clusters of *s*-*p* bonded metals and strong chemical interactions between Al and Au atoms.

The Al_{13}^- cluster is electronically equivalent to the neutral magic cluster $Al_{12}Si$ and it is possible to form the symmetric compound neutral fullerene $Si@Al_{12}Au_{20}$ in which the capping Al atoms become closer to Si, with Al-Si and Au-Si bond lengths being 3.97 and 3.99 Å, respectively. The Au-Au bonds are slightly elongated to 2.85 Å, while the Al-Au bond lengths are shorter with the value of 2.56 Å. The HOMO-LUMO gap is nearly the same with the value of 0.54 eV. There could be a number of other possibilities of forming compound fullerenes such as $Cu_{12}Au_{20}$ and $Ag_{12}Au_{20}$ that are isoelectronic to Au_{32}. Both Cu-Au and Ag-Au alloys have an ordering tendency in bulk. We find that the HOMO-LUMO gaps of Cu-Au and Ag-Au fullerenes are 1.12 and 1.49 eV, while the BEs are 2.406 and 2.080 eV/atom, respectively. Therefore, energetically the $Al_{12}Au_{20}$ fullerene is very significantly lower in energy and it is the best among the systems we have studied. We also tried $Li_{12}Au_{20}$ and it has similar BE as Au_{32} but the HOMO-LUMO gap is only 0.46 eV.

IV. SUMMARY

In summary we have reported the findings of a compound fullerene $Al_{12}Au_{20}$ and an endohedral compound fullerene $Al@Al_{12}Au_{20}$ constituted from metal atoms. These are new examples of fullerenes formed of metal atoms. These are highly stable with large heats of formation. The HOMO-LUMO gap in these fullerenes is smaller compared with that in Au_{32}, and there are interesting possibilities as the structures of the cation and neutral $Al@Al_{12}Au_{20}$ fullerenes show movement of Al atoms inside and outside the Au cage. In chemical reactions, often a charge transfer is involved and such clusters could be a dynamical system for catalytic reactions. It is also possible that similar cage structures could exist for other elements. Recently we have shown[18] that fullerene structures can also be formed between Al and transition metals such as Pt and Pd. In the case of Pt, small clusters favor open structures[19] similar to the case of Au and alloying provides the possibility of forming other structures with high dispersion to make new catalysts. We hope that our finding would encourage experimentalists to produce these compound fullerenes in the laboratory.

Note added in proof. The stability of the $Al_{12}Au_{20}$ cage is further supported from calculations on $Au@Al_{12}Au_{20}^-$ which has a fivefold symmetric cage structure with the endohedral Au atom drifting towards the wall of the cage below an Al atom. This 58–valence electron species (leaving aside the 5*d* electrons of Au atoms) has special stability with a large HOMO-LUMO gap of 0.99 eV. The $Al_{12}Au_{20}$ cage can accommodate a few more atoms and these results will be published separately.

ACKNOWLEDGMENTS

I am grateful to the staff of the Center for the Development of Advanced Computing for allowing the use of the Param Padam supercomputing facility and their excellent support. Financial support from the U.S. Asian Office of Aerospace Research and Development is thankfully acknowledged.

[1] H. Kroto, J. Heath, S. O'Brien, R. Curl, and R. Smalley, Nature (London) **318**, 162 (1985).
[2] B. C. Guo, K. P. Kerns, and A. W. Castleman, Jr., Science **255**, 1411 (1992); B. C. Guo, S. Wei, J. Purnell, S. Buzza, and A. W. Castleman, Jr., *ibid.* **256**, 515 (1992).
[3] M. P. Johansson, D. Sundholm, and J. Vaara, Angew. Chem., Int. Ed. **43**, 2678 (2004); X. Gu, M. Ji, S. H. Wei, and X. G. Gong, Phys. Rev. B **70**, 205401 (2004); M. Ji, X. Gu, X. Li, X. G. Gong, J. Li, and L.-S. Wang, Angew. Chem., Int. Ed. **44**, 7119 (2005).
[4] N. Gonzalez Szwacki, A. Sadrzadeh, and B. I. Yakobson, Phys. Rev. Lett. **98**, 166804 (2007).
[5] See Q.-B. Yan, X.-L. Sheng, Q.-R. Zheng, L.-Z. Zhang, and G. Su, Phys. Rev. B **78**, 201401(R) (2008), and references therein.
[6] S. Bulusu, X. Li, L. S. Wang, and X. C. Zeng, Proc. Natl. Acad. Sci. U.S.A. **103**, 8326 (2006).
[7] X. P. Xing, B. Yoon, U. Landman, and J. H. Parks, Phys. Rev. B **74**, 165423 (2006).
[8] J. Li, X. Li, H. J. Zhai, and L. S. Wang, Science **299**, 864 (2003).
[9] M. Haruta, Catal. Today **36**, 153 (1997); M. D. Hughes, Y.-J. Xu, P. Jenkins, P. McMorn, P. Landon, D. I. Enache, A. F. Carley, G. A. Attard, G. J. Hutchings, F. King, E. H. Stitt, P. Johnston, K. Griffin, and C. J. Kiely, Nature (London) **437**, 1132 (2005).
[10] W. A. de Heer, Rev. Mod. Phys. **65**, 611 (1993).
[11] V. Kumar, K. Esfarjani, and Y. Kawazoe, in *Clusters and Nanomaterials: Theory and Experiment*, edited by Y. Kawazoe, T. Kondow, and K. Ohno (Springer, Heidelberg, 2002).
[12] X. G. Gong and V. Kumar, Phys. Rev. Lett. **70**, 2078 (1993).

[13] R. E. Leuchtner, A. C. Harms, and A. W. Castleman, Jr., J. Chem. Phys. **91**, 2753 (1989); **94**, 1093 (1991).
[14] V. Kumar, S. Bhattacharjee, and Y. Kawazoe, Phys. Rev. B **61**, 8541 (2000).
[15] G. Kresse and D. Joubert, Phys. Rev. B **59**, 1758 (1999); P. E. Blöchl, *ibid.* **50**, 17953 (1994).
[16] J. P. Perdew, in *Electronic Structure of Solids '91*, edited by P. Ziesche and H. Eschrig (Akademie, Berlin, 1991).
[17] L. Pauling, Proc. Natl. Acad. Sci. U.S.A. **36**, 533 (1950).
[18] V. Kumar (unpublished).
[19] V. Kumar and Y. Kawazoe, Phys. Rev. B **77**, 205418 (2008).